Tribology International 123 (2018) 43–49

Contents lists available at ScienceDirect

Tribology International

journal homepage: www.elsevier.com/locate/triboint

Numerical investigations on drag coefficient of circular cylinder with two free ends in roller bearings

Wenjun Gao [a,b,*], Daniel Nelias [a], Yaguo Lyu [b], Nicolas Boisson [a]

[a] Univ Lyon, INSA-Lyon, CNRS, UMR5259, LaMCoS, F-69621, France
[b] School of Power and Energy, Northwestern Polytechnical University, Xi'an, China

ARTICLE INFO

Keywords:
Drag coefficient
Roller bearing
Reynolds number
Numerical simulation

ABSTRACT

In high speed roller bearings, the drag force due to the oil-air mixture present in the bearing cavity – that is acting against the roller movement – is usually computed with a two-dimensional model of flow around a cylinder of infinite length. However rollers are of finite length, and the flow is perturbed by the two free ends, the surrounding rings, the cage and other rolling elements. In this article, the Computational Fluid Dynamics (CFD) method is employed to analyze first the flow around one finite-length circular cylinder with two free ends in an open space. Then the model is changed to one finite cylinder and then several in-line circular cylinders sandwiched by two flat walls, which represents a simplified approach. The results indicate that both the flow pattern around the cylinder and its drag coefficient are modified in comparison with the two-dimensional model. Finally a relationship between the drag coefficient and the Reynolds number suitable for circular cylinder in roller bearings is proposed.

1. Introduction

In a rotating machinery system like turbine engine, roller bearings play an important role in supporting the rotating shaft or rotor, and need lubrication to insure their function. In the bearing, only a small quantity of oil is needed to form the elastohydrodynamic lubricant (EHL) film in the contact zone, the EHL film thickness being less than a few tenth of micrometer. Most of lubricant remains in suspension in air, forming an oil/air mixture like a fog, which contributes to cool down the bearing components [1] – with an effect somewhat proportional to the oil flow – but also acts as a heat source for high speed applications with an increase of dissipation roughly proportional to the square of the rotational speed. This phenomenon leads to excessive parasitic hydraulic losses when rolling elements translate and rotate into the fluid environment, which may constitute a relatively large portion of the bearing's total power loss, named drag or windage loss. For high speed applications, i.e. for rotational speed up to $3\times\ 10^6\ Ndm$, the contribution of drag/windage loss to the total one may reach up to 50% [2,3]. This can be easily observed with a test bench by measuring the input shaft torque when shutting off the oil feed. A simple model has been introduced by Harris [4] for estimating the drag force acting on the roller, based on the solution for one isolated body in translation into a one phase fluid:

$$F_r = \frac{1}{2} C_d \rho V^2 A \tag{1}$$

where F_r is the drag force (N), ρ the mass density of the fluid (kg/m^3), V the velocity at which the body is traveling (m/s), and A the frontal area of the body to the flow direction (m^2). Here the drag coefficient C_d plays a dominant part in the drag force calculation. It is plotted in Fig. 1 as a function of the Reynolds number, both for a smooth cylinder and a smooth sphere [5].

This approach is however too simplified since interactions with the roller surrounding are neglected. This has been the purpose of recent investigations for ball bearings. Marchesse et al. [6] and Pouly et al. [7] experimentally proved that the drag coefficient for spheres in ball bearings is nearly divided by a factor 5 in comparison with that for an isolated sphere. In their research the effect of rings is ignored, which is a strong simplification as pointed out by Yan et al. [8]. Very recently the latest authors correlated experimental observations in high-speed ball bearings and 3D CFD computations [9], emphasizing that the flow performance strongly depends also on the lubricant supply method in addition to the internal bearing geometry. Meantime high-speed roller bearings have received less attention. The relationship between the drag coefficient and the Reynolds number plotted in Fig. 1 for cylinder is obtained for an infinitely long roller, i.e. without free ends. While the circular cylinder in

* Corresponding author. School of Power and Energy, Northwestern Polytechnical University, Xi'an, China.
E-mail address: wenjun.gao@insa-lyon.fr (W. Gao).

https://doi.org/10.1016/j.triboint.2018.02.044
Received 15 December 2017; Received in revised form 19 February 2018; Accepted 26 February 2018

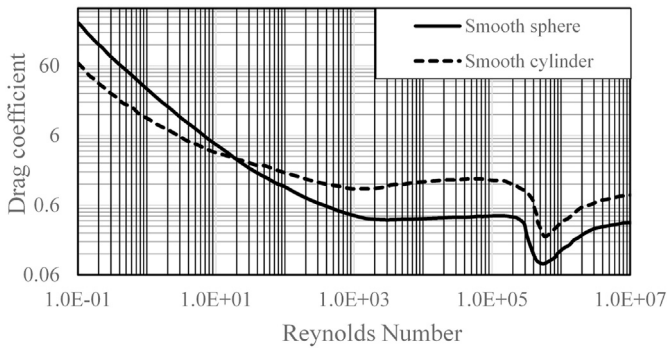

Fig. 1. Drag coefficient of ideal sphere and circular cylinder by Schlichting [5].

roller bearings is of finite-length with two free-side ends immersed into a viscous fluid. The shear flow that separates from free ends may interact violently with that from the cylindrical surface and results in a three-dimensional flow phenomenon [10], as shown in Fig. 2. Not only that, but the cylinder is sandwiched by two rings with micron-size clearance so that the oil-air mixture could only bypass the free ends rather than the cylindrical surface. Moreover, with relative short gap between two adjacent rollers, flow around several in-line cylinders could interact with each other, like that in ball bearings [11,12]. Consequently, the drag coefficient for cylindrical elements in roller bearings has to be investigated with a three-dimensional model and should take the surrounding rings and rollers into account (see Fig. 3).

In this article, a CFD model is proposed to study the flow pattern around a circular cylinder with two free ends without and with nearby walls as in roller bearings in order to clarify the effect of the geometry on the drag force acting on its surface. First one isolated circular cylinder in an open space is simulated and compared with experimental data to verify the model. After that, the model is employed to investigate one isolated cylinder and further several in-line cylinders sandwiched by two flat walls. Vortex flow around the finite-length cylinder in different configurations is revealed and a new relationship of drag coefficient varying with the Reynolds number suitable for cylindrical elements in roller bearings is obtained. Note that the same methodology could be easily applied to more complex geometrical and kinematical configurations such as high-speed gearboxes [14,15], for example.

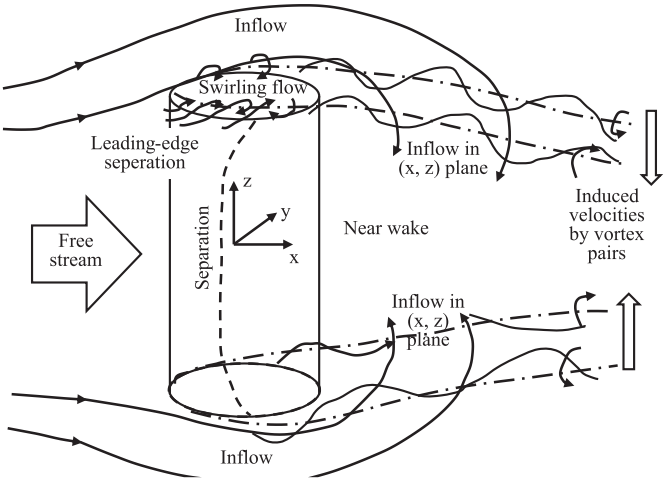

Fig. 2. Sketch of flow around a circular cylinder with two free ends [13].

2. Numerical approach

2.1. Numerical computation domain

In roller bearings, a series of cylindrical roller elements transfer through the oil-air mixture periodically, together with the cage and surrounded by the inner and outer rings. To clarify flow characteristics around the roller, the problem is simplified to a series of finite-length circular cylinders transferring into a one phase flow. The effect of the cage is ignored because it has been demonstrated experimentally that their effect is of second order on the drag coefficient value [16]. Three different configurations are established and studied for a cylinder of finite length: 1) Configuration #1 considers one isolated circular cylinder in an open space. Its center is located 5 times the cylinder diameter (5D) downstream of the inlet and 15D upstream of the outlet. The other four sides are 5D far from the center of the cylinder. 2) Configuration #2 ignores the ring's curvature and considers one isolated cylinder sandwiched by two flat walls, with micron-size clearance between the cylindrical surface and the flat walls. 3) Configuration #3 considers three sandwiched circular cylinders in tandem with periodic boundary condition, instead of endless circular cylinders orbiting in the bearing. The referred roller bearing specifications are given in Table 1.

All three fluid domains are meshed with structured hexahedron grids with the commercial software ANSYS ICEM. In order to avoid low mesh quality, the radial clearance between the cylinder and the walls is assumed here two times bigger than that in a real bearing. In the contact regions, there is a minimum of 6 elements between the clearance at 10 levels of refinement. The average y^+ (the dimensionless wall distance) is in the range $y^+ < 5$ on the walls, in order to capture the near-wall turbulent region in a transient calculation. To match this requirement for all calculation cases, much finer cells are used around the cylinder, with about 1.25 million cells in the configuration #1 and 2.9 million cells for the configurations #2 and 3.

2.2. Governing equations

When the roller transfers through the oil-air two phase flow in bearing cavity, a shear stress is produced by the gradients of velocity at the roller surface with no-slip condition. The shear stress sums to one part of the total drag force exerting on the roller called the viscous drag. Besides, the pressure of the fluid is greater on the front of roller than that on the backside, which introduces the other part, called the pressure drag or form drag [17].

To catch detailed shear stress and pressure distribution around the cylinder in high Reynolds number, the SST Scale-Adaptive Simulation (SAS) model is used, with the SIMPLEC pressure-velocity coupling method. The SST SAS model explicitly adds a von Karman length scale to the turbulence RANS model to dynamically adjust to resolved structures in a URANS simulation, which results in a LES-like behavior in unsteady flow field. At the same time, the model provides standard RANS capabilities in stable flow regions [18].

The governing equations of the SST SAS model are followed,

$$\frac{\partial \rho k}{\partial t} + \nabla\cdot(\rho U k) = P_k - \rho c_\mu k\omega + \nabla\cdot\left[\left(\mu + \frac{\mu_t}{\sigma_k}\right)\nabla k\right] \tag{2}$$

$$\frac{\partial \rho \omega}{\partial t} + \nabla\cdot(\rho U \omega) = \alpha\frac{\omega}{k}P_k - \rho\beta\omega^2 + Q_{SAS} + \nabla\cdot\left[\left(\mu + \frac{\mu_t}{\sigma_\omega}\right)\nabla\omega\right] + (1-F_1)\frac{2\rho}{\sigma_{\omega 2}}\frac{1}{\omega}\nabla k\nabla\omega \tag{3}$$

where

$$Q_{SAS} = max\left[\rho\zeta_2\kappa S^2\left(\frac{L}{L_{vk}}\right)^2 - C\cdot\frac{2\rho k}{\sigma_\Phi}max\left(\frac{|\nabla\omega|^2}{\omega^2}, \frac{|\nabla k|^2}{k^2}\right), 0\right] \tag{4}$$